

COMPUTATIONAL STUDY OF NADH INTERACTIONS WITH VOLTAGE  
DEPENDENT ANION CHANNEL

By  
SAI SHASHANK CHAVALI

A thesis submitted to the  
Graduate School-Camden  
Rutgers, State University of New Jersey  
  
In partial fulfillment of the requirements  
For the degree of Masters of Science  
Graduate Program in Biology  
  
Written under the direction of  
Dr. Grace Brannigan

And approved by

---

Dr. Jessica Grace Brannigan

---

Dr. Eric Klein

---

Dr. William M. Saidel

Camden, New Jersey  
July 2016

## Thesis Abstract

### Computational Study of Small Molecule Interaction with Voltage Dependent Anion Channel

by SAI SHASHANK CHAVALI

Dissertation Director:  
Dr. Grace Brannigan

The Voltage Dependent Anion Channel (VDAC) is a mitochondrial outer membrane protein that serves as a diffusion pore for ions like  $Ca^{2+}$ ,  $Cl^-$ , small metabolites and nucleotides like ATP, ADP and NADH, thereby regulating metabolic and energetic flux across the outer mitochondrial membrane. Previous studies have indicated that Nicotinamide adenine dinucleotide in its reduced form (NADH) but not oxidized form (NAD $^+$ ) minimizes conduction through VDAC. However, there is no available non-conducting structure of VDAC, and the mechanism by which NADH modulates the channel is poorly understood. Here with the help of fully-atomistic molecular dynamics simulations, we studied NADH binding to VDAC and its effect on channel dynamics and ion translocation. Simulations of VDAC were conducted using NMR structure of VDAC-NADH complex a) in the presence of NADH, and with NADH bound as in that structure, b) de-protonated in silico to NAD $^+$  and c) removed entirely (apo) in the presence and absence of an applied transmembrane voltage. We observed a constant dissociation and re-association of NAD $^+$  throughout the simulation trajectory, while NADH remained bound, reflecting a significantly lowered

affinity of NAD<sup>+</sup> for the VDAC pore. In the apo-VDAC system, the N-terminal loop dramatically changed its conformation over the course of the simulation, eventually approaching its conformation in structures experimentally determined in an apo-state. Under an applied transmembrane potential, we observed NADH changing its position, but remaining stable in the pore. Our results are consistent with a mechanism in which NADH reduces conduction by partial pore block.

# Contents

<b>1</b>	<b>Introduction</b>	<b>1</b>
1.1	Voltage Dependent Anion Channel . . . . .	1
1.2	Structure and Permeation through VDAC . . . . .	3
1.3	VDAC - NADH . . . . .	4
1.4	Molecular Dynamics . . . . .	5
1.4.1	MD simulations - Background . . . . .	5
<b>2</b>	<b>Methods</b>	<b>7</b>
2.1	NMR structure of VDAC-NADH complex . . . . .	7
2.2	MD Simulations System Setup . . . . .	8
2.3	Simulation Details . . . . .	10
2.4	Trajectory Analysis . . . . .	11
2.4.1	Figure Preparation and Statistics . . . . .	11
<b>3</b>	<b>Results</b>	<b>12</b>
3.1	Ligand and VDAC dynamics . . . . .	12

3.1.1	NADH's stability in the pore . . . . .	12
3.1.2	NAD+’s transient nature in the pore . . . . .	14
3.1.3	Conformational change of N-terminal loop in the VDAC-Apo state . . . . .	15
3.2	Pore block by NADH . . . . .	17
3.3	Simulations under membrane potential - VDAC(N) . . . . .	18
3.3.1	NADH’s movement in the pore under transmembrane voltage . . . . .	18
3.3.2	Pore hydration in the presence and absence of transmembrane voltage . . . . .	20
<b>4</b>	<b>Discussion</b>	<b>22</b>
<b>5</b>	<b>Acknowledgment</b>	<b>24</b>

# List of Figures

1.1	VDAC	2
1.2	NADH and NAD+	2
1.3	VDAC open probability vs Voltage (mv)	5
2.1	NMR structures of VDAC-NADH complex	8
2.2	VDAC complexes used for MD	9
2.3	System generated by CHARMM-GUI	10
3.1	NADH RMSD and Hydrogen bond plots	12
3.2	NAD+ RMSD and Hydrogen bond plots	14
3.3	RMSD - N-terminal loop of VDAC(P)-Apo	15
3.4	Pore hydration plot for VDAC(P) systems	17
3.5	Z-Height of NADH in VDAC(N)-NADH complex	18
3.6	Pore hydration plot for VDAC(N) systems	20

# Chapter 1

## Introduction

### 1.1 Voltage Dependent Anion Channel

The role of mitochondria in cellular respiration, signaling of apoptotic factors and metabolite transportation has been well established. These metabolites have to cross two membrane barriers, an inner and outer membrane. The inner membrane is selective and permeable only to oxygen, water and carbon di oxide and is folded into layers called cristae. The outer membrane is composed of protein-based pores that facilitate the transfer of ions, metabolites and small proteins to and from the mitochondria. Voltage dependent anion channel (VDAC) is one such pore, that serves as a channel for metabolites and ion exchange between the cytoplasm and the mitochondria[13][3]. VDAC is the most abundant protein in the mitochondrial outer membrane and is shown to be responsible for mitochondrial-mediated cell death in pathological conditions like cancer, Alzheimer's, and Parkinson's, and hence VDAC has emerged as a promising pharmacological target[27][26]. It is also debated that VDAC is expressed in the cell surface membrane[25][4][16].

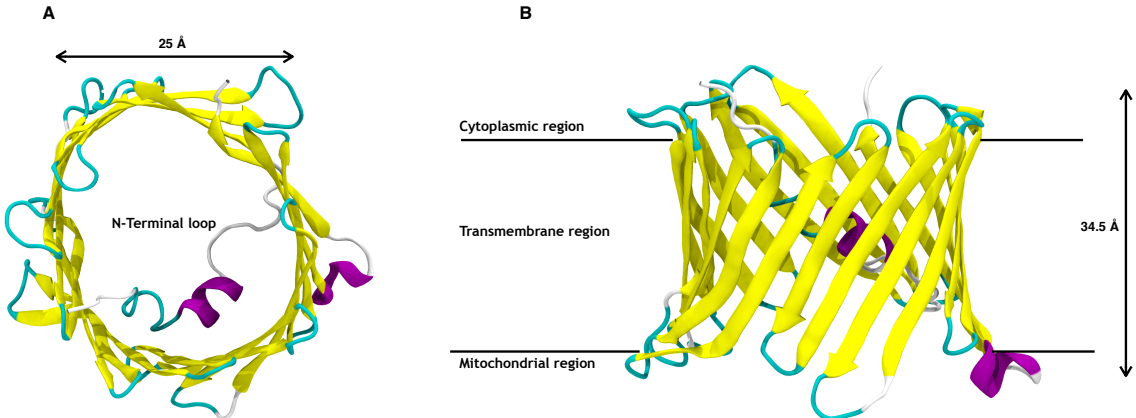


Figure 1.1: **VDAC** Cartoon representation of VDAC structure from (A) cytoplasmic and (B) transmembrane view. Protein is colored by secondary structure ( $\beta$  sheet=yellow,  $\alpha$  helix=purple and loop=cyan)

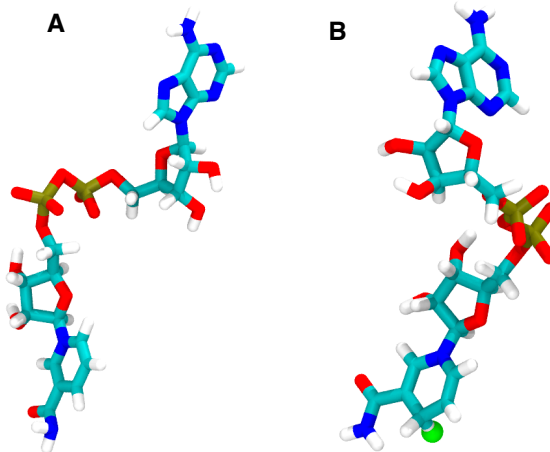


Figure 1.2: **NADH and NAD<sup>+</sup>** Nicotinamide adenine dinucleotide phosphate is a coenzyme that is involved in metabolism, carrying electrons from one reaction to another and hence is found as (A) NAD<sup>+</sup>, an oxidizing agent that accepts electrons from other molecules and becomes (B) NADH (extra hydrogen represented in green Vdw representation), a reducing agent that donates the electron to other molecules and . The molecules are colored by atom type, White : Hydrogen, Blue : Nitrogen, Cyan : Carbon, Red : Oxygen and Tan : Phosphorous

VDAC not only acts as a pathway for the transfer of small ions like  $Ca^{2+}, K^+, Na^+, Cl^-$  or water soluble metabolites like NADH, ATP, ADP and pyruvate but was also shown to translocate monomeric  $\alpha$ -synuclein[21] and oligomerize to conduct cytochrome

C[28] during apoptosis. Recent advancements in structural determination using nuclear magnetic resonance[7] and X-ray crystallography[30], opened doors to structure-based prediction of VDAC's functional properties.

## 1.2 Structure and Permeation through VDAC

The 3-dimensional structures of mammalian VDAC determined using X-ray crystallography and NMR revealed that VDAC is a 280 amino acid long,  $\beta$ -barrel structure composed of 19  $\beta$  strands[7] with the transmembrane  $\alpha$ -helix oriented against the inner wall[30]. The X-ray and NMR studies (native structures)[6] of VDAC were shown to adopt a diameter of 27 $\text{\AA}$  and a height of 30 $\text{\AA}$  with similar charge distributions. There is a 26 residue loop attached to the N-terminal segment of the protein. Both the NMR and crystal structure discuss the structural importance of the N-terminal loop in the gating of VDAC.

VDAC reconstituted into planar lipids (non-native) was solely used to understand the ion permeation process in VDAC. VDAC allows a variety of molecules to pass through the pore. Its permeability is dependent on the charge of the molecules. VDAC attains its highest conducting state at low or zero membrane potential, the open state, where it is selective to negatively charged molecules[19][20]. It adopts a closed conformation at membrane potentials in excess of -30mv and 30mv[1]. However a structural understanding of the "closed state" of VDAC remains a "terra incognita". Nucleotides like ATP and NADH, unlike small ions, may specifically in-

teract with charged residues on the interior wall. VDAC was also shown to have an ATP-binding site[20].

Rapid development in sampling methods[22][14] [23] and robust hardware solutions[5] helped in extracting thermodynamic and kinetic information of ion channels through molecular dynamics simulations[32][15][29]. These recent studies provide a better understanding of VDAC's structural behavior and conduction properties. Long time scale molecular dynamics simulations have been used to study ion transport[12], ATP flux [17][2] through VDAC, mechanisms underlying its electrophysiology properties[24] and its interaction with cholesterol[31].

### 1.3 VDAC - NADH

There are a number of stimuli known to favor the gating of VDAC. Altered membrane potential is a prime consequence. Zizi M et al., in electrophysiology studies showed that VDAC's (reconstituted into planar membranes) interacts with Nicotinamide adenine dinucleotide in its reduced form (NADH) but not oxidized form (NAD+), thereby minimizing conduction through VDAC[33]. It was later suggested that the presence of NADH mimics membrane potentials (-30mv and 30mv) that closes the channel.

Though there is evidence suggesting the role of NADH in reduced ion conduction through VDAC, there is no available non-conducting state of VDAC; and the mechanism by which NADH modulates the channel is poorly understood. Does NADH induce conformational changes in VDAC, thereby affecting the ion transloca-

tion through the channel or is it NADH's steric presence that induces partial pore blockage, are the main questions addressed in this study. With the help of fully-atomistic molecular dynamics simulations, we studied NADH binding to VDAC and its effect on channel dynamics and ion translocation. A 3-D structure of VDAC-NADH complex obtained through Nuclear Magnetic Resonance (personal communication with Dr. Sebastian Hiller) was used to carry out molecular dynamics simulations.

Figure 1.3: **VDAC open probability vs Voltage (mv)** An open probability of human VDAC1 as a function of voltage in the presence (filled diamonds) and absence (control - open squares) of NADH. NADH seems to slow down the probability of opening the channel[33].

## 1.4 Molecular Dynamics

### 1.4.1 MD simulations - Background

Molecular dynamics simulations is a robust technique used to systematically study molecular conformations by combining traditional equations of motion over a period of time. The main purpose of this approach is to produce results that reflect the time-dependent behavior (dynamics) of a molecule. A detailed atomistic understanding of interactions between biological complexes, cannot be observed through experimental procedures today. Molecular dynamics simulations has a broad spectrum of appli-

cations where atomic interactions, inter-residue interactions, folding and unfolding pathway of proteins and binding affinities of small molecules and ligands to proteins can be understood. An exponential increase in computational resources now allows researchers to simulate large systems like ion channels, transporters and even cell organelles like ribosomes to enable a partnership with experimental research, delivering structural insights into complex biological problems. In addition, MD simulations also allow us to test a specific hypothesis based on experimental study.

The aim of this study is to understand the mechanism by which NADH reduces ion conduction through VDAC. A time-dependent structural behavior of NADH in the VDAC pore can answer questions related to the role of NADH in VDAC closure. This can be achieved by atomistic molecular dynamics simulations, where VDAC-NADH binding is studied under an atomic resolution.

# Chapter 2

## Methods

### 2.1 NMR structure of VDAC-NADH complex

Previous NMR structure of Apo-VDAC (PDB ID: 2K4T) was determined by S.Hiller et al[7] in 2009. This structure has been previously used to perform molecular dynamics studies on VDAC to understand ion permeation through the channel[24]. However, there was no experimentally determined structure to study NADH mediated ion conduction through VDAC. Dr. Sebastian Hiller's lab at University of Basel have determined the structure of VDAC in the presence of NADH using solid state nuclear magnetic resonance. A preliminary structure of the VDAC-NADH complex was determined where NADH to VDAC is docked by 10 NOEs (Nuclear Overhauser Effect), generated during the experiment, that defined the contact and position of the nicotinamide moiety of NADH. A later structure of the VDAC-NADH complex was resolved under a better resolution. Both these structures were used to perform molecular dynamics simulations.

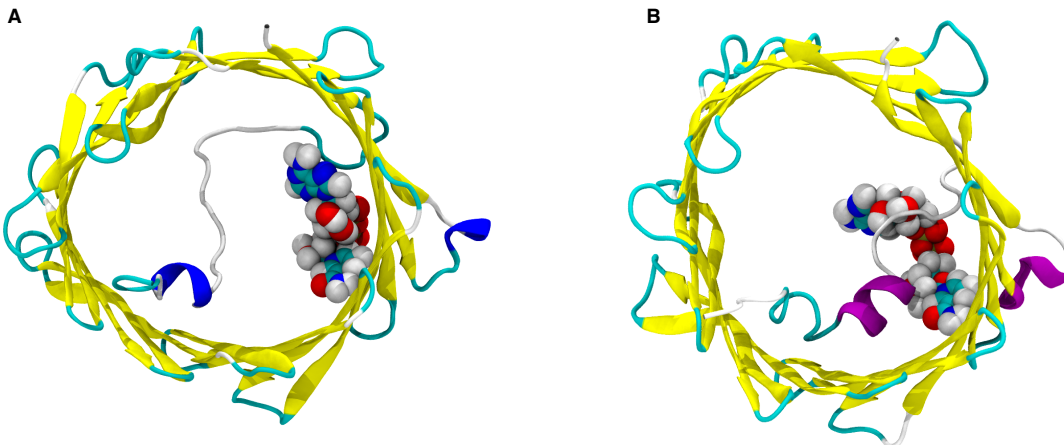


**Figure 2.1: NMR structures of VDAC-NADH complex**(A) Preliminary NMR structure of VDAC-NADH complex (B) Newly resolved NMR structure of VDAC-NADH complex. The newly resolved structure has a better resolved alpha helix and altered NADH binding site.

## 2.2 MD Simulations System Setup

With the aim of understanding conduction through VDAC in the presence and absence of NADH and NAD<sup>+</sup> (as a negative control), the preliminary structure of VDAC bound to NADH was deprotonated and removed completely using Visual Molecular Dynamics (VMD) v1.9.2[8] to generate VDAC-NAD<sup>+</sup> and VDAC-Apo states respectively. The new structure was also modified in silico to generate VDAC systems in the presence and absence of NADH and NAD<sup>+</sup>. In addition these systems were simulated under a transmembrane voltage of -30mv. The protein was oriented along the z-axis, normal to the membrane. CHARMM-GUI membrane builder[9] was used to build the membrane for all the three systems (VDAC bound to NADH, NAD<sup>+</sup> and

VDAC Apo). CHARMM36 topology and parameter files were manually uploaded to generate membranes for VDAC-NADH and VDAC-NAD<sup>+</sup> systems.

System label	Expt Method	Ligand (Experimental state)	Ligand (Computational state)
Preliminary structure			
VDAC(P)-Apo	NMR	NADH	Removed in silico
VDAC(P)-NADH	NMR	NADH	NADH
VDAC(P)-NAD <sup>+</sup>	NMR	NADH	Deprotonated to NAD <sup>+</sup>
New structure			
VDAC(N)-Apo	NMR	NADH	Removed in silico
VDAC(N)-NADH	NMR	NADH	NADH
VDAC(N)-NAD <sup>+</sup>	NMR	NADH	Deprotonated to NAD <sup>+</sup>
Crystal structure			
3EMN	X-Ray	Apo	-

Table 1 : Details of the systems used for molecular dynamics and analysis

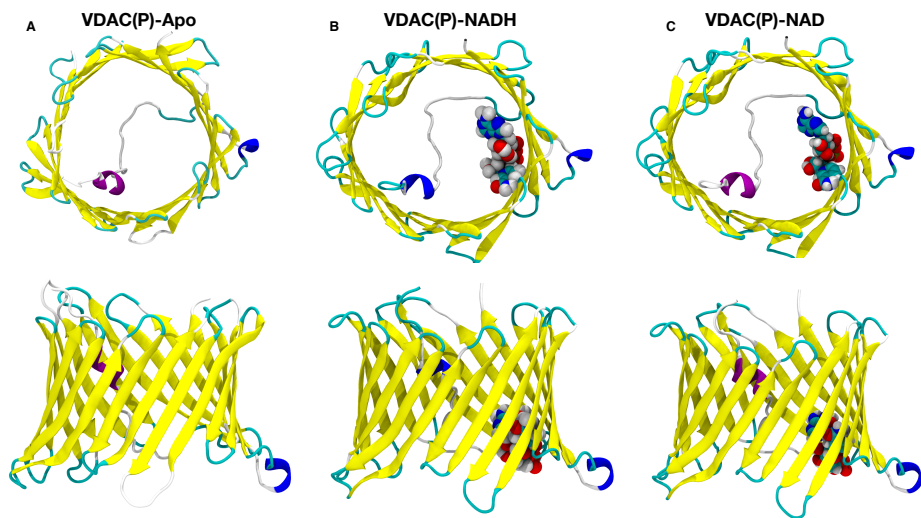
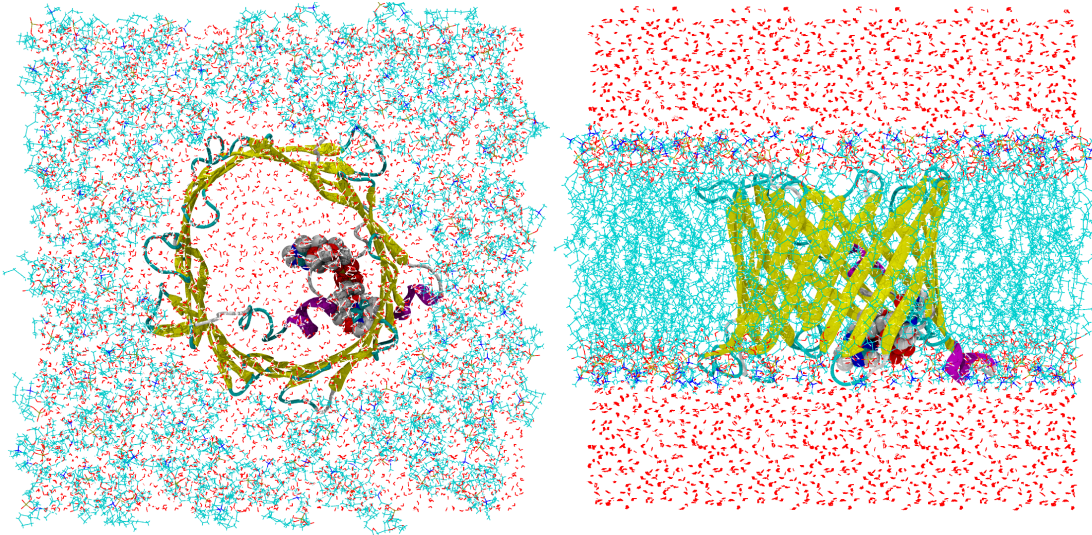


Figure 2.2: **VDAC complexes used for MD** Structure of VDAC(P) from cytoplasmic (top) and transmembrane (bottom) views for the NMR systems. (A) VDAC(P)-Apo (B) VDAC(P)-NADH (C) VDAC(P)-NAD<sup>+</sup>. Protein and ligands are shown as cartoon and vdW representations, respectively.



**Figure 2.3: System generated by CHARMM-GUI VDAC(N)-NADH system used for simulation generated by CHARMM-GUI with approximately 11000 water molecules and 150 DOPC molecules**

28 K<sup>+</sup> and Cl<sup>-</sup> ions were randomly added by CHARMM-GUI to neutralize the system and provide a salt concentration of 0.15M KCl. The lipid bilayer for all the systems are composed of DOPC (1,2-Dioleoyl-sn-glycero-3-phosphocholine) molecules. KCl is generally favored over NaCl in VDAC experiments to minimize the effects of ionic size and diffusivity on measurements. The resulting systems were approximately 84 x 84 x 84 Å<sup>3</sup> in size, with about 60000 atoms (for VDAC-NADH and NAD<sup>+</sup>) and 56000 atoms (for VDAC-Apo) that included about 11000 TIP3P waters.

## 2.3 Simulation Details

Atomistic molecular dynamics simulations for all the systems were carried out using NAMD v2.10[18]. VMD was used to visualize and analyze the trajectories. Periodic

boundary conditions and Particle Mesh Ewald (PME) electrostatics were used for all the simulations. A Langevin thermostat and barostat were used to maintain a temperature and pressure of 303.15 K and 1 atm, respectively and no surface tension was imposed. The simulation time step was 2 fs. All the systems were equilibrated for 6 ns each to gradually release restraints on the protein. In total, 3 separate simulations totaling about  $4.5 \mu\text{ s}$  ( $1.5 \mu\text{ s}$  per system) contributed to this work.

## 2.4 Trajectory Analysis

Production simulations were analyzed with VMD[8]. The trajectories were wrapped and aligned to the backbone before the following analyses was conducted:

- RMSD: RMSD trajectory tool in VMD was used to calculate the root mean square deviation of the C-alpha atoms of the protein and ligands (heavy atoms).
- Pore hydration: A Tcl script was used to calculate the water molecules in the channel radius throughout the trajectory and along the Z axis.
- Hydrogen bonds: Hydrogen bonds were calculated with the hydrogen bond plugin of VMD with a  $3.3 \text{ \AA}^3$  and  $20^\circ$  donor–acceptor cutoff diffusion.

### 2.4.1 Figure Preparation and Statistics

Structural figures and movies of the systems were generated with VMD. The RMSD and hydrogen bond plots were generated using Xmgrace plotting tool. Pore hydration plots were generated using python.

# Chapter 3

## Results

### 3.1 Ligand and VDAC dynamics

#### 3.1.1 NADH's stability in the pore

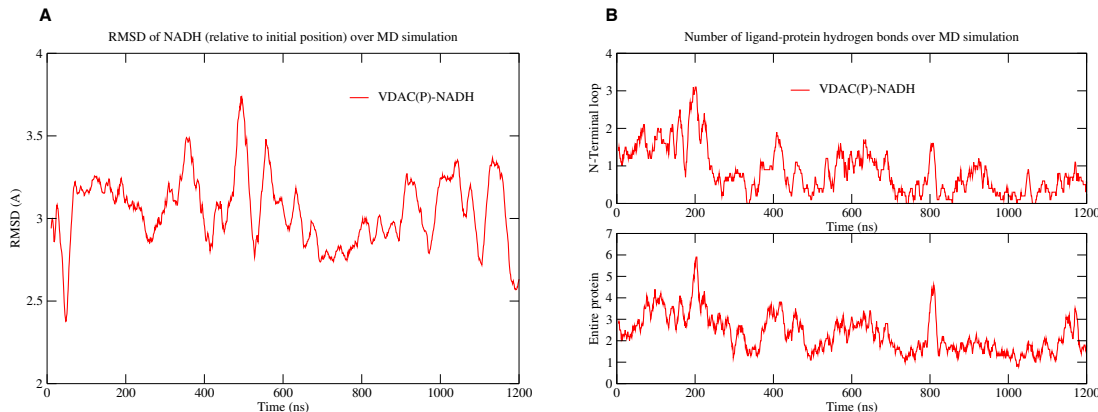
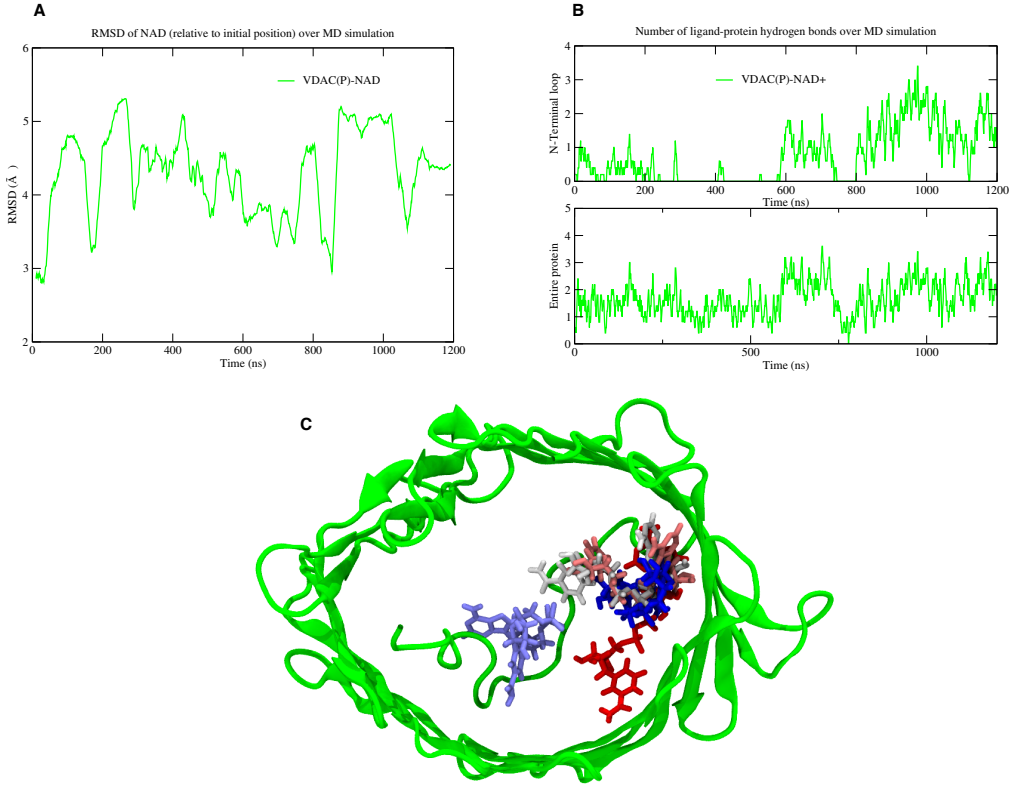


Figure 3.1: **Ligand RMSD and Hydrogen bond plots** (A) RMSD of NADH in  $\text{\AA}$ , indicating its stability inside the pore (B) Hydrogen bond plot showing NADH's stable interaction with the N-terminal loop and the entire protein.

We used the NMR structure of VDAC(P)-NADH complex for simulations that ran for 1.2  $\mu$  seconds. NADH (with no hydrogens included) in the due course of the simulation stayed anchored to its initial binding site with an average root square de-

vation of 3Å(Fig 3.1 A ). NADH also forms stable hydrogen bonds with the protein and N-terminal loop (Fig 3.1 B). Electrophysiology studies that suggest NADH mediated reduction in conduction, also emphasizes on the role of NADH's stability in the pore[33]. Therefore NADH's stability is indispensable to understand the mechanism by which NADH mediates VDAC pore block and the simulation trajectories consistently display NADH stability in the pore.

### 3.1.2 NAD<sup>+</sup>'s transient nature in the pore



**Figure 3.2: NAD<sup>+</sup> RMSD and Hydrogen bond plots** (A) RMSD of NAD in Å, indicating its transient nature inside the pore (B) Hydrogen bond plot showing NAD's unstable interaction with the N-terminal loop and the entire protein (C) A snapshot of the VDAC(P)-NAD<sup>+</sup> system along the Z axis showing the conformational distribution of NAD<sup>+</sup> along the trajectory, from Red (initial conformations) through Gray (middle conformations) to Blue (final conformations). NAD<sup>+</sup> over the due course of the simulation moves towards the N-Terminal and returns to its original position.

NAD<sup>+</sup> is the oxidized form of NADH and it was experimentally shown to bring about no significant change in conduction through VDAC[33]. The NMR structure of VDAC(P)-NADH was modified in silico to generate VDAC-NAD<sup>+</sup> system, which was used to run simulations that ran for 1.2  $\mu$  seconds. NAD<sup>+</sup> in the due course of

the simulation, exhibits transient behavior. NAD<sup>+</sup> (heavy atoms) RMSD shows its inconsistent positioning in the channel (Fig 3.2 A).

NAD<sup>+</sup> also forms fluctuating hydrogen bonds with the N-Terminal loop and the entire protein (Fig 3.2 B). These results consistently strengthens the experimental study that shows NADH, but not NAD<sup>+</sup> minimizes conduction through VDAC.

### 3.1.3 Conformational change of N-terminal loop in the VDAC-

#### Apo state

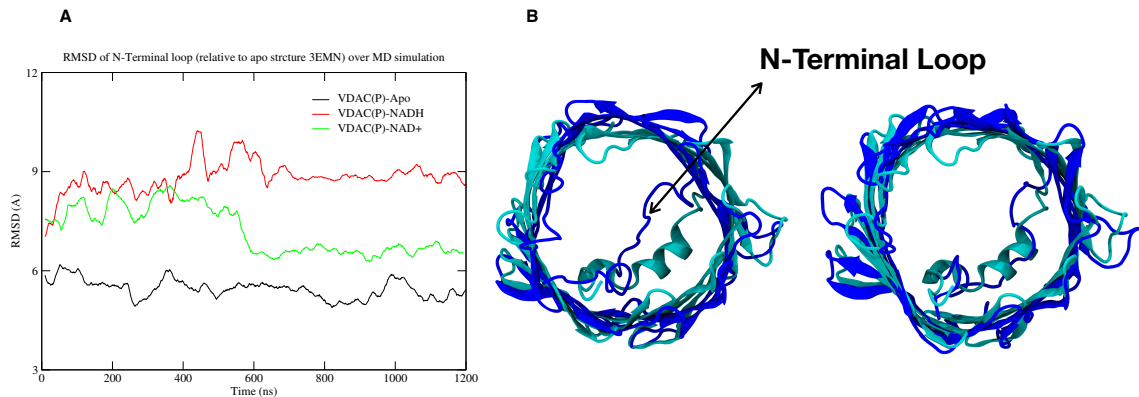


Figure 3.3: **RMSD - N-terminal loop of VDAC(P)-Apo** (A) RMSD of N-Terminal loop aligned to the crystal structure. Following the removal of NADH in silico from the initial NADH structure (black curve), VDAC(P) conformation approached that of a structure determined in an experimental apo state (PDB ID: 3EMN) (B) (left) Snapshot of the first frame of NMR-Apo system (Blue) aligned with the experimental apo state (Cyan). (Right) is the snapshot of the same system after 500 ns.

The VDAC-Apo system was generated by removing NADH from the NMR structure of the VDAC-NADH complex in silico. The N-terminal loop in the VDAC-Apo system prior to the simulation is positioned in the center of the pore due to the presence of NADH, however in the due course of the simulation, the N-terminal loop changes

its orientation and reaches the experimentally determined position. The RMSD of the N-terminal loop of the VDAC-Apo system reduces when the experimentally determined VDAC structure (PBD ID: 3EMN) is made the reference (Fig 3.3 A) protein. This is consistent with the earlier experimental observation[30][7] that confirmed the orientation of the N-terminal loop in the pore.

### 3.2 Pore block by NADH

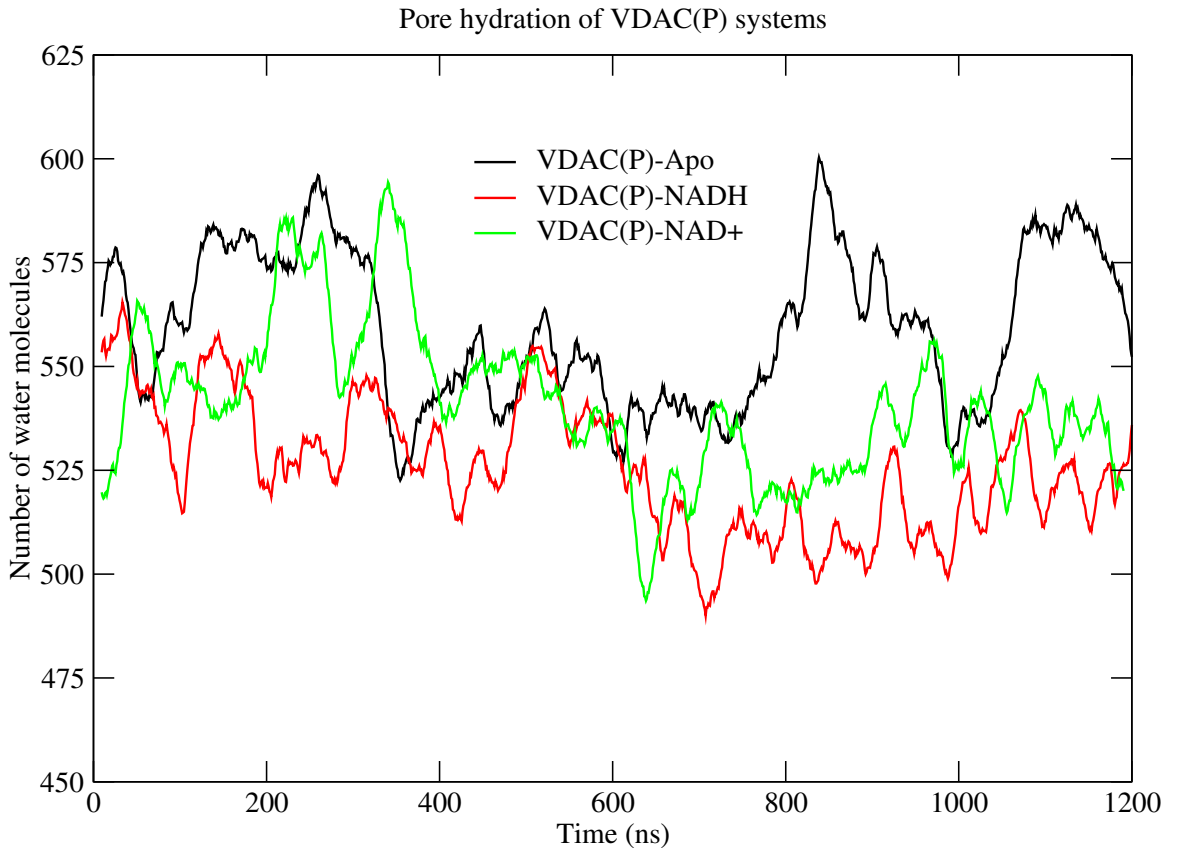


Figure 3.4: **Pore hydration plot for VDAC(P) systems**  
 Count of water molecules inside the channel for the three VDAC systems vs. time. A reduction in the number of water molecules in the VDAC-NADH system was observed when compared to the other VDAC systems. NADH occupies a volume of approximately  $2400 \text{ \AA}^3$  which is equivalent to 80 water molecules.

NADH is a 72-atom nucleotide that occupies a substantial volume ( $2400 \text{ \AA}^3$ ) in the pore. Hence to confirm whether the steric presence of NADH minimizes conduction through VDAC the number of water molecules that pass through the channel throughout the simulation has been plotted (Fig 3.5).

NADH occupies a volume that is equivalent to 80 water molecules and a decrease

in the number of water molecules in the presence of NADH was observed when compared to the apo protein. In addition, NAD<sup>+</sup>'s instability in the pore resulted in inconsistent pore occupancy that was reflected in the pore hydration plot. This plot therefore confirms that the steric presence of NADH is responsible for the diminished conductance through VDAC.

### 3.3 Simulations under membrane potential - VDAC(N)

#### 3.3.1 NADH's movement in the pore under transmembrane voltage

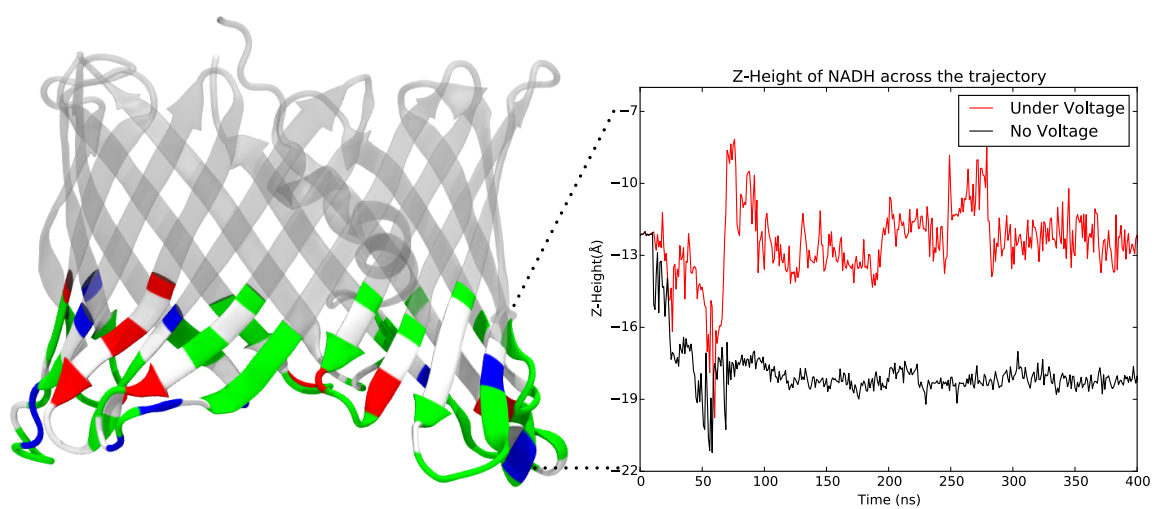
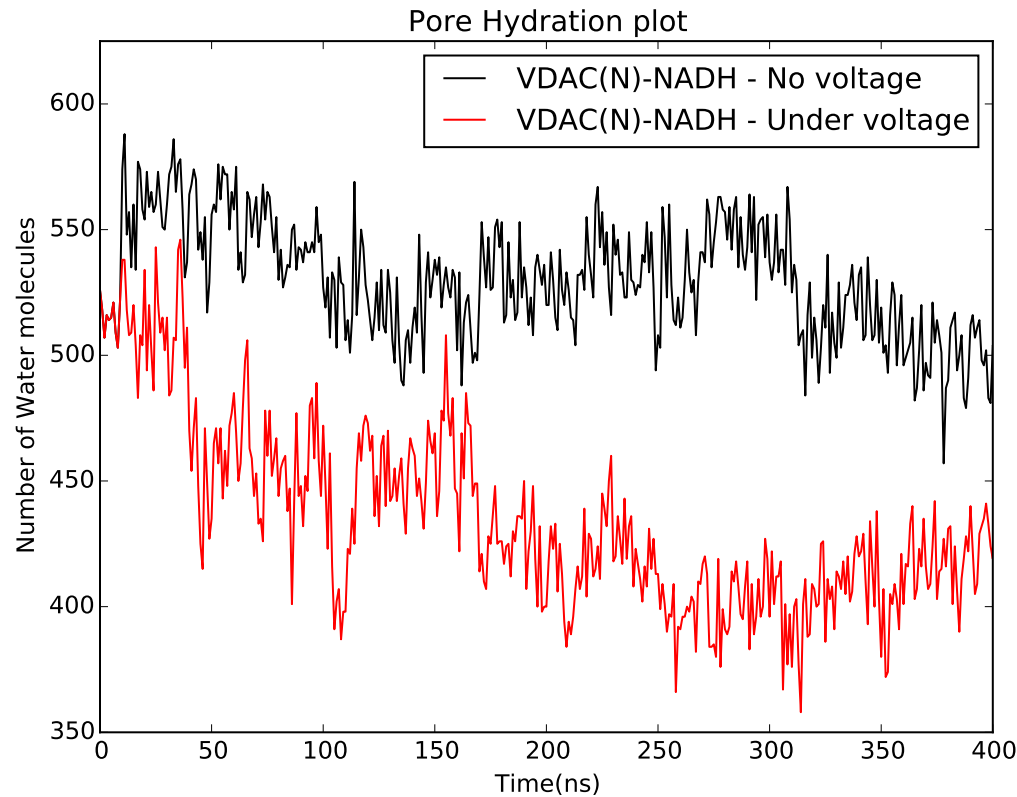


Figure 3.5: **Z-Height of NADH in VDAC(N)-NADH complex** Movement of NADH through the Z axis in the simulations with VDAC(N)-NADH complex under an applied transmembrane voltage. NADH, shifts from its initial binding site in the due course of the simulation but stays inside the pore. Under no applied voltage it localizes near the N-terminus region throughout the simulation appearing to be leaving the channel.

The opening and closing of VDAC is dependent on voltage[19][20]. Experimental studies on VDAC-NADH complex were performed under an applied transmembrane voltage[33][11][10]. Hence the NMR structure of the VDAC(N)-NADH complex was used for simulations under an applied transmembrane voltage of -30mV. NADH's mobility in the pore is significant under an applied transmembrane voltage. NADH, in the first 100 ns of the simulation leaves its initial binding site and moves across the channel to reach the opposite end (Fig 3.5). NADH carries a negative charge of -2 and its movement from the initial binding site can be explained by a repulsion with the negative charge created by the transmembrane potential. Though NADH is quite mobile under an applied transmembrane voltage, post 100 ns, it remains more stable in its new site. This region of the protein has charged residues and stability can be explained by a electrostatic interactions of NADH with the charged residues in the protein. In addition under no applied transmembrane voltage, NADH shifts from its initial binding site and localizes near the N-terminal region giving an impression of leaving the pore. The Z-Height plot (Fig 3.5, black plot) indicates the Z coordinates ( $\text{\AA}$ ) of NADH across the trajectory, where NADH moves from its initial binding site in the first 50 ns. Post 50 ns, it localizes around the N-terminus region (at approximately -18  $\text{\AA}$ ) for the rest of the trajectory. When compared to the preliminary structure, the orientation of the N-terminal loop and NADH is altered in the new structure. The NOEs that define the binding site in the preliminary structure seem to be varying in the new structure. This variation could be a reason for NADH's differed behavior in the new structure.

### 3.3.2 Pore hydration in the presence and absence of trans-membrane voltage



**Figure 3.6: Pore hydration plot for VDAC(N) systems** Movement of NADH through the Z axis in the simulations with VDAC(N)-NADH complex under an applied transmembrane voltage. NADH, shifts from its initial binding site in the due course of the simulation but stays inside the pore.

The pore hydration plot (Fig 3.4) confirms that NADH occupancy in the pore influences conduction through VDAC. Fig 3.6 shows the number of water molecules through out the trajectory for the VDAC(N)-NADH system with and without an applied transmembrane voltage. Fig 3.4 shows the movement of NADH under no applied transmembrane potential, where NADH is localizes in the N-terminus region.

The number of water molecules throughout the trajectory in this case is reduced when compared to NADH's presence in the pore under an applied transmembrane voltage. This supports the idea that NADH's steric presence in the pore minimizes conduction through the channel. Moreover the experimental studies suggest that NADH reduces and increases the open channel probability of VDAC at -30 mV and 0 mV respectively. [33]. The pore hydration plot (Fig 3.6) with VDAC(N)-NADH complex is more consistent with the experimental observations.

# Chapter 4

## Discussion

With the help of the fully atomistic molecular dynamics simulations, we observe the mechanism of NADH mediated pore block in VDAC. The structure used for the simulations was experimentally determined using nuclear magnetic resonance in the presence of NADH and hence has a potential binding site. Though NADH was known to reduce conduction through VDAC, it was unknown whether NADH brings about conformational changes in VDAC to reduce conductance or just blocks the pore. Our results are consistent with the observation that NADH minimizes conduction through VDAC by partially blocking the channel due to its steric presence. The pore hydration plots provide crucial evidence to support the above observation, where the number of water molecules passing through the pore across the simulation is less in the presence of NADH.

Our results are also consistent with experimental observations that suggest NAD<sup>+</sup> having no effect on conduction through VDAC. In the due course of the simulation we observed NAD<sup>+</sup> dissociating and re-associating reflecting an inconsistent pore hydration plot. The VDAC-Apo system used for simulation was generated by computationally removing NADH from the VDAC-NADH complex. In the due course

of the simulation the N-terminal loop shifts its position and reaches the experimentally determined orientation. The pore hydration plot for the VDAC-Apo system showed increased number of water molecules throughout the trajectory that bolsters our NADH mediated pore block observation.

# Chapter 5

## Acknowledgment

I would like to thank Dr. Sebastian Hiller, University of Basel, for providing the NMR structure of the VDAC-NADH complex.

Funding:NIH P01GM55876-14A1, Computational resources:NSF XSEDE Allocation NSF-MCB110149 and local cluster funded by NSF-DBI1126052

# Bibliography

- [1] Elizabeth Blachly-Dyson and Michael Forte. Vdac channels. *IUBMB life*, 52(3-5):113–118, 2001.
- [2] Om P Choudhary, Aviv Paz, Joshua L Adelman, Jacques-Philippe Colletier, Jeff Abramson, and Michael Grabe. Structure-guided simulations illuminate the mechanism of atp transport through vdac1. *Nature structural & molecular biology*, 21(7):626–632, 2014.
- [3] Marco Colombini. Vdac: the channel at the interface between mitochondria and the cytosol. *Molecular and cellular biochemistry*, 256(1-2):107–115, 2004.
- [4] Vito De Pinto, Angela Messina, Darius JR Lane, and Alfons Lawen. Voltage-dependent anion-selective channel (vdac) in the plasma membrane. *FEBS letters*, 584(9):1793–1799, 2010.
- [5] JP Grossman, Jeffrey S Kuskin, Joseph A Bank, Michael Theobald, Ron O Dror, Douglas J Ierardi, Richard H Larson, U Ben Schafer, Brian Towles, Cliff Young, et al. Hardware support for fine-grained event-driven computation in anton 2. *ACM SIGARCH Computer Architecture News*, 41(1):549–560, 2013.
- [6] Sebastian Hiller, Jeff Abramson, Carmen Mannella, Gerhard Wagner, and Kornelius Zeth. The 3d structures of vdac represent a native conformation. *Trends in biochemical sciences*, 35(9):514–521, 2010.
- [7] Sebastian Hiller, Robert G Garces, Thomas J Malia, Vladislav Y Orekhov, Marco Colombini, and Gerhard Wagner. Solution structure of the integral human membrane protein vdac-1 in detergent micelles. *Science*, 321(5893):1206–1210, 2008.
- [8] William Humphrey, Andrew Dalke, and Klaus Schulten. VMD – Visual Molecular Dynamics. *Journal of Molecular Graphics*, 14:33–38, 1996.
- [9] Sunhwan Jo, Taehoon Kim, Vidyashankara G Iyer, and Wonpil Im. Charmm-gui: a web-based graphical user interface for charmm. *Journal of computational chemistry*, 29(11):1859–1865, 2008.
- [10] An-Chin Lee, Xiaofeng Xu, and Marco Colombini. The role of pyridine dinucleotides in regulating the permeability of the mitochondrial outer membrane. *Journal of Biological Chemistry*, 271(43):26724–26731, 1996.

- [11] An-Chin Lee, Martin Zizi, and Marco Colombini. Beta-nadhl decreases the permeability of the mitochondrial outer membrane to adp by a factor of 6. *Journal of Biological Chemistry*, 269(49):30974–30980, 1994.
- [12] Kyu Il Lee, Huan Rui, Richard W Pastor, and Wonpil Im. Brownian dynamics simulations of ion transport through the vdac. *Biophysical journal*, 100(3):611–619, 2011.
- [13] John J Lemasters and Ekhson Holmuhamedov. Voltage-dependent anion channel (vdac) as mitochondrial governor—thinking outside the box. *Biochimica et Biophysica Acta (BBA)-Molecular Basis of Disease*, 1762(2):181–190, 2006.
- [14] Adam Liwo, Cezary Czaplewski, Stanisław Ołdziej, and Harold A Scheraga. Computational techniques for efficient conformational sampling of proteins. *Current opinion in structural biology*, 18(2):134–139, 2008.
- [15] Robert T McGibbon and Vijay S Pande. Learning kinetic distance metrics for markov state models of protein conformational dynamics. *Journal of Chemical Theory and Computation*, 9(7):2900–2906, 2013.
- [16] Christian Niehage, Charlotte Steenblock, Theresia Pursche, Martin Bornhäuser, Denis Corbeil, and Bernard Hoflack. The cell surface proteome of human mesenchymal stromal cells. *PLoS One*, 6(5):e20399, 2011.
- [17] Sergei Yu Noskov, Tatiana K Rostovtseva, and Sergey M Bezrukov. Atp transport through vdac and the vdac–tubulin complex probed by equilibrium and nonequilibrium md simulations. *Biochemistry*, 52(51):9246–9256, 2013.
- [18] James C Phillips, Rosemary Braun, Wei Wang, James Gumbart, Emad Tajkhorshid, Elizabeth Villa, Christophe Chipot, Robert D Skeel, Laxmikant Kale, and Klaus Schulten. Scalable molecular dynamics with namd. *Journal of computational chemistry*, 26(16):1781–1802, 2005.
- [19] Tatiana Rostovtseva and Marco Colombini. Atp flux is controlled by a voltage-gated channel from the mitochondrial outer membrane. *Journal of Biological Chemistry*, 271(45):28006–28008, 1996.
- [20] Tatiana Rostovtseva and Marco Colombini. Vdac channels mediate and gate the flow of atp: implications for the regulation of mitochondrial function. *Biophysical journal*, 72(5):1954, 1997.
- [21] Tatiana K Rostovtseva, Philip A Gurnev, Olga Protchenko, David P Hoogerheide, Thai Leong Yap, Caroline C Philpott, Jennifer C Lee, and Sergey M Bezrukov.  $\alpha$ -synuclein shows high affinity interaction with voltage-dependent anion channel, suggesting mechanisms of mitochondrial regulation and toxicity in parkinson disease. *Journal of Biological Chemistry*, 290(30):18467–18477, 2015.

- [22] Benoit Roux, Toby Allen, Simon Berneche, and Wonpil Im. Theoretical and computational models of biological ion channels. *Quarterly reviews of biophysics*, 37(01):15–103, 2004.
- [23] Benoît Roux, Simon Bernèche, Bernhard Egwolf, Bogdan Lev, Sergei Y Noskov, Christopher N Rowley, and Haibo Yu. Ion selectivity in channels and transporters. *The Journal of general physiology*, 137(5):415–426, 2011.
- [24] Huan Rui, Kyu Il Lee, Richard W Pastor, and Wonpil Im. Molecular dynamics studies of ion permeation in vdac. *Biophysical journal*, 100(3):602–610, 2011.
- [25] Ravshan Z Sabirov and Petr G Merzlyak. Plasmalemmal vdac controversies and maxi-anion channel puzzle. *Biochimica et Biophysica Acta (BBA)-Biomembranes*, 1818(6):1570–1580, 2012.
- [26] Varda Shoshan-Barmatz and Danya Ben-Hail. Vdac, a multi-functional mitochondrial protein as a pharmacological target. *Mitochondrion*, 12(1):24–34, 2012.
- [27] Varda Shoshan-Barmatz, Vito De Pinto, Markus Zweckstetter, Ziv Raviv, Nurit Keinan, and Nir Arbel. Vdac, a multi-functional mitochondrial protein regulating cell life and death. *Molecular aspects of medicine*, 31(3):227–285, 2010.
- [28] Varda Shoshan-Barmatz, Nurit Keinan, Salah Abu-Hamad, Dalia Tyomkin, and Lior Aram. Apoptosis is regulated by the vdac1 n-terminal region and by vdac oligomerization: release of cytochrome c, aif and smac/diablo. *Biochimica et Biophysica Acta (BBA)-Bioenergetics*, 1797(6):1281–1291, 2010.
- [29] Diwakar Shukla, Carlos X Hernández, Jeffrey K Weber, and Vijay S Pande. Markov state models provide insights into dynamic modulation of protein function. *Accounts of chemical research*, 48(2):414–422, 2015.
- [30] Rachna Ujwal, Duilio Cascio, Jacques-Philippe Colletier, Salem Faham, Jun Zhang, Ligia Toro, Peipei Ping, and Jeff Abramson. The crystal structure of mouse vdac1 at 2.3 Å resolution reveals mechanistic insights into metabolite gating. *Proceedings of the National Academy of Sciences*, 105(46):17742–17747, 2008.
- [31] Brian P Weiser, Reza Salari, Roderic G Eckenhoff, and Grace Brannigan. Computational investigation of cholesterol binding sites on mitochondrial vdac. *The Journal of Physical Chemistry B*, 118(33):9852–9860, 2014.
- [32] Fangqiang Zhu and Gerhard Hummer. Convergence and error estimation in free energy calculations using the weighted histogram analysis method. *Journal of computational chemistry*, 33(4):453–465, 2012.
- [33] Martin Zizi, Mike Forte, Elizabeth Blachly-Dyson, and Marco Colombini. NADH regulates the gating of vdac, the mitochondrial outer membrane channel. *Journal of Biological Chemistry*, 269(3):1614–1616, 1994.